Optimization of the Wind Turbine Layout and Transmission System Planning for a Large-Scale Offshore Wind Farm by AI Technology

Yuan-Kang Wu, *Member, IEEE*, Ching-Yin Lee, Chao-Rong Chen, *Senior Member, IEEE*, Kun-Wei Hsu, and Huang-Tien Tseng

***Abstract*—The interest in the utilization of offshore wind power is increasing significantly worldwide. A typical offshore wind farm may have hundreds of generators, which is outspread in the range of several to tens of kilometers. Therefore, there are many feasible schemes for the wind turbine location and internal line connection in a wind farm. The planner must search for an optimal one from these feasible schemes, usually with a maximum wind power output and the lowest installation and operation cost. This paper proposes a novel procedure to determine the optimization wind turbine location and line connection topology by using artificial intelligence techniques: The genetic algorithm is utilized in the optimal layouts for the offshore wind farm, and the ant colony system algorithm is utilized to find the optimal line connection topology. Furthermore, the wake effect, real cable parameters, and wind speed series are also considered in this research. The concepts and methods proposed in this study could help establish more economical and efficient offshore wind farms in the world.**

***Index Terms*—Ant colony system (ACS), artificial intelligence, genetic algorithm (GA), offshore wind power, optimization, wake effect.**

I. Introduction

THE INTEREST in the utilization of offshore wind power is increasing significantly worldwide. The offshore wind power potential can be considered to be significant. In Europe, the theoretical potential is estimated to lie between 2.8 and 3.2 PWh and up to 8.5 PWh [1]. However, investment costs for offshore wind power are much higher than those for onshore installations. Generally, the electrical system of an offshore wind farm is composed of a local collection system, an integration system, a transmission system, and a grid interface. Currently, offshore wind farms tend to be bigger, and the distance between wind turbines is usually greater than that in onshore wind farms because of the larger wake effect offshore. For large offshore wind farms, higher voltage levels will certainly be useful in order to minimize power losses, but higher voltage levels may result in bigger transformers and higher costs for these transformers. Therefore, the internal electric system of an offshore wind farm and its connection to the main power system pose new challenges.

A typical offshore wind farm may have hundreds of generators, which are outspread in the range of several to tens of kilometers, so that, at a certain reliability level, there are many feasible schemes for each wind turbine location and the internal electric connection system in a wind farm. The wind farm planner must search for an optimal one from the feasible schemes. It should be noted that such optimization is of much significance. For example, the cost of an internal electric connection system is about 8% of the total investment costs for an onshore wind farm, while the proportion is 18% for an offshore one [2]. Therefore, optimization of the internal electric connection system for wind farms, particularly for offshore ones, will remarkably improve the economy.

There are several papers that discuss about the optimization of a wind farm [3]–[9]: In [3], the development of a tool, evolutionary algorithms, is introduced to optimize the individual turbine sitting and the electricity infrastructure by considering the costs of equipment and production losses due to the wake effect. Reference [4] proposed a model for optimizing ac electric power systems of offshore wind farms, which covers investment costs, system efficiency, and system reliability. Reference [5] introduces a new probabilistic optimization methodology to the problem of optimal positioning of turbines in a wind farm by considering a set of possible scenarios and their probability of occurrence. Reference [6] focuses on the planning of an offshore wind farm power grid in Taiwan, and several case studies are reported. Reference [7] evaluates the electrical system of offshore wind farms by considering system reliability. The work in [8] studies the collector system design problem with a graph-theoretic approach building upon classical graph-theoretic algorithms. Reference [9] proposes a clustering-based cable layout configuration, in which three different cable layout configurations have been compared from the perspectives of overall cost, system reliability, and system real power losses.

Manuscript received June 26, 2012; revised March 9, 2013; accepted September 1, 2013. Date of publication September 24, 2013; date of current version May 15, 2014. Paper 2012-ESC-235.R1, presented at the 2012 IEEE Industry Applications Society Annual Meeting, Las Vegas, NV, USA, October 7–11, and approved for publication in the IEEE Transactions on Industry Applications by the Energy Systems Committee of the IEEE Industry Applications Society.

Y.-K. Wu is with the Department of Electrical Engineering, National Chung Cheng University, Chiayi 62102, Taiwan (e-mail: allenwu@ccu.edu.tw).

C.-Y. Lee is with Tungnan University, Taipei 222, Taiwan, and also with the Department of Electrical Engineering, National Taipei University of Technology, Taipei 106, Taiwan (e-mail: cylee@mail.tnu.edu.tw).

C.-R. Chen is with the Department of Electrical Engineering, National Taipei University of Technology, Taipei 106, Taiwan (e-mail: crchen@ntut.edu.tw; t7318006@ntut.edu.tw).

K.-W. Hsu is with Taiwan Power Company, Taipei 100, Taiwan (e-mail: sean.y2k@yahoo.com.tw).

H.-T. Tseng is with Taiwan Semiconductor Manufacturing Company, Hsinchu 30078, Taiwan (e-mail: damage224@hotmail.com).

Color versions of one or more of the figures in this paper are available online at http://ieeexplore.ieee.org.

Digital Object Identifier 10.1109/TIA.2013.2283219

Various genetic algorithm (GA) technologies have been widely proposed for optimizing offshore wind farms [10]–[15]. For instance, an advanced model for optimizing the electric power system by using the GA technology has been reported in [10], where the power losses, wind power production, initial investment, and maintenance costs are considered. Another optimization method based on a hybrid genetic and immune algorithm has been presented in [11]. Additionally, the performance of several GA techniques has been evaluated in [12]–[14].

In addition to GAs, several other methods have also been proposed for optimizing offshore wind farms [16]–[20]: In [16], an artificial neural network model was developed to estimate the optimal number of wind turbines and the total produced power in a wind farm. In [17], an improved Gaussian particle swarm optimization (PSO) algorithm is proposed to optimize the positions of turbines. Reference [18] introduces a new tool, based on the net present value, for optimizing wind turbine locations in large offshore wind farms. In [19], the authors describe the design of a multiobjective PSO algorithm to act as a wind farm layout optimization module. Reference [20] presents an ant colony algorithm for maximizing the expected energy output. The algorithm considers wake loss, which can be calculated based on wind turbine locations, and wind direction.

In a large wind farm, the wake effect among turbines cannot be ignored, and wind turbine arrangement must be reasonably selected to reduce air flow interaction among turbines. If the space among wind turbines is too small, the impact of the wake effect from upwind turbines to downwind turbines will be greater, resulting in the reduction of the generating output of downwind turbines. Several research works have focused on this topic [21]–[25]: In [21], an approach to the optimization of large wind farms is presented, which considers wake superposition. In [22], a GA approach is employed to obtain optimal placement of wind turbines for maximum generation output while limiting the number of installed turbines. In [23], several impact factors on the wind farm layout such as topography and wake are analyzed, and the model is established to maximize the economic benefits. Reference [24] briefly outlines the wind turbine wakes and describes a numerical model to calculate the wake flow field. Comparison of experimental data with model calculations is used to draw conclusions about the wake flow field in [25].

Although several research works have discussed about the optimization design for offshore wind farms, most of them only focus on the determination of wind turbine location. The main contribution of this paper is to consider not only wind turbine location but also internal line connection to form a complete planning for offshore wind farms.

This paper focuses on the impact of wake effects and lists a wind turbine construction location diagram that will achieve maximum wind farm efficiency. After the construction of the wind turbines, the wind farm's internal cable distribution is configured. In this work, the wake effect between wind turbines will be considered, and the GA will be utilized in the optimal layouts for the wind farm. Additionally, the ant colony system (ACS) algorithm will be utilized to find the optimal line connection for the radial-type topology. The proposed method in this paper would provide a significant reference to future offshore wind farm planning.

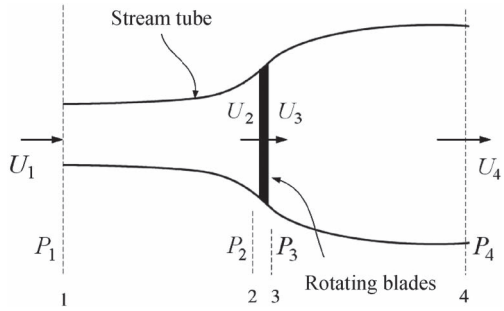

Fig. 1. Tube model for the rotor flow.

II. Momentum Theory

Momentum theory can be used to describe the relationship between wind force power on the rotor and flow velocity and how much mechanical energy can be converted from wind energy. By using the 1-D momentum equation in Fig. 1, one can obtain thrust T on the rotor as

$$T = m(U_1 - U_4) \tag{1}$$

where U_1 is the upstream velocity from the front of the rotor, U_4 is the wake velocity behind the rotor, and m is the air mass flow through the rotor and can be represented as

$$m = \rho U_2 A \tag{2}$$

where ρ is the air density, A is the area swept by the rotor, and U_2 is the velocity of the flow through the rotor.

By substituting m in (2) into (1), one can obtain

$$T = \rho A U_2 (U_1 - U_4). \tag{3}$$

According to the momentum theory, the axial force T on the rotor can be expressed as

$$T = A(P_2 - P_3). \tag{4}$$

It is assumed that air pressures far in front and behind the rotor are equal; using the Bernoulli equation one can obtain

$$P_2 - P_3 = 0.5\left(U_1^2 - U_4^2\right). \tag{5}$$

Substitution into (4) can obtain

$$T = 0.5\rho A\left(U_1^2 - U_4^2\right). \tag{6}$$

By (3) and (6), one can obtain

$$U_2 = 0.5(U_1 + U_4). \tag{7}$$

Here, the axial induction factor is defined as $a = U_a/U_1$, where U_a is the axial induction velocity on the rotor; then,

$$U_2 = U_1(1 - a) \tag{8}$$

$$U_4 = U_1(1 - 2a). \tag{9}$$

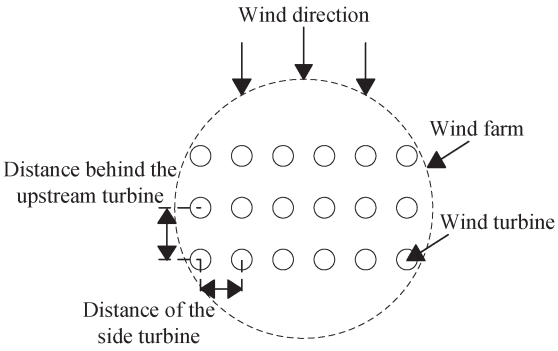

Fig. 2. Wind farm array diagram.

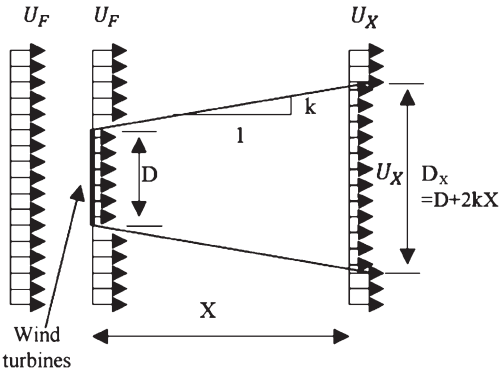

Fig. 3. Wake effect diagram.

Additionally, the axial induction factor can be expressed as

$$a = 0.5(1 - U_4/U_1). \tag{10}$$

From (6) and (9), the following new equation is obtained:

$$T = 2a\rho AU_1^2(1-a). \tag{11}$$

The rotor thrust coefficient C_T is defined as

$$C_T = 2T/\rho AU_1^2. \tag{12}$$

Bringing (11) into (12),

$$C_T = 4a(1-a). \tag{13}$$

The rotor's absorption power P equals the difference in air flow kinetic energy in the front and back of the rotor

$$P = 0.5m\left(U_1^2 - U_4^2\right) = 0.5\rho AU_2\left(U_1^2 - U_4^2\right). \tag{14}$$

Bring (8) and (9) into (14) to obtain

$$P = 2\rho AU_1^3 a(1-a)^2. \tag{15}$$

The rotor power coefficient C_P is defined as

$$C_P = 2P/\rho AU_1^3. \tag{16}$$

Bring (15) into (16) to obtain

$$C_P = 4a(1-a)^2. \tag{17}$$

Therefore, the rotor power coefficient $C_{P\max} \approx 0.593$ is greatest when $a = 1/3$. This value is called Betz's extreme limit.

Aside from wind velocity, wind power parameters also need to consider wind direction due to the impact of the wake effect. Fig. 2 shows the diagram for a wind farm array.

According to Katic's derivative model [26], the area affected by the wake effect will gradually expand following the lengthening of the distance between two wind turbines, but the strength of the effect will gradually decrease, as shown in Fig. 3.

Wind velocity will be influenced by wind farm topography, such as surface roughness, undulating terrain, and artificial buildings. Surface roughness is also called roughness length. Surface roughness length is an important parameter in the study of atmospheric environment and air flow mechanics. The value of the roughness length depends on the height and spacing of surface obstacles. Table I introduces the roughness level, length, and wake decay constant of various terrain features.

TABLE I
VARIOUS TERRAIN FEATURES

Terrain category	Roughness level	Roughness length (m)	Wake decay constant, k
Maritime	0.0	0.0002	0.040
Mixed land and water zone	0.5	0.0024	0.052
Farmland	1.0 ~ 2.0	0.03 ~ 0.1	0.063~0.083
Trees and farmland	2.5	0.20	0.092
Forest and village	3.0	0.40	0.100
Large town or city	3.5	0.80	0.108
Large city	4.0	1.60	0.117

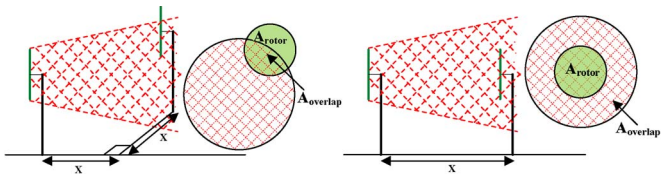

Fig. 4. Shaded area owing to wake effect.

It can be seen through Fig. 3 that a downwind turbine is affected by the upwind turbine's wake, and the effect area is A_{overlap}, as shown in Fig. 4. If the upwind turbine's wind velocity is U_F and its distance to the downwind turbine is X meters, then the downwind velocity is U_X. Then deriving in accordance with the principle of conservation of momentum, the reduction of wind velocity between downwind and upwind turbines is [14]

$$\begin{aligned} dV &= U_F - U_X \\ &= U_F \cdot (1 - \sqrt{1 - C_T}) \cdot (D/(1+2kX))^2 \\ &\quad \cdot (A_{\text{overlap}}/A_{\text{rotor}}) \end{aligned} \tag{18}$$

where D is the diameter of the upwind turbine blade, X is the distance between the axes of the upwind and downwind rotors, and k is the wake decay constant.

The shaded area in different cases, such as Figs. 5 and 6, can be calculated by using (19) and (20), which are derived from geometric principles. Here, $A_{\text{overlap}} = A_1 + A_2$.

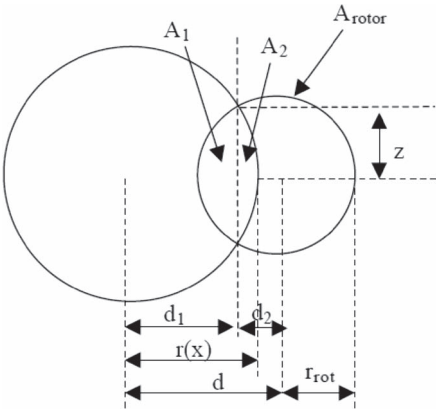

Fig. 5. Shaded area calculated by $d = d_1 + d_2$.

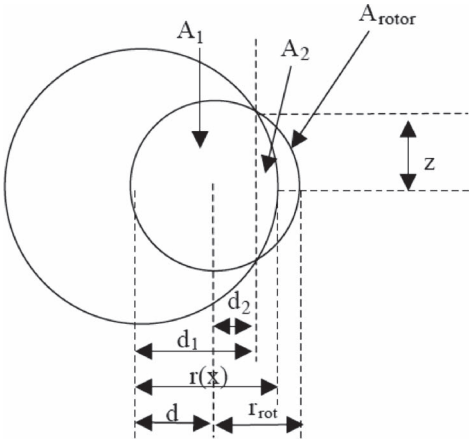

Fig. 6. Shaded area calculated by $d = d_1 - d_2$.

As shown in Fig. 5, when $d = d_1 + d_2$,

$$\begin{aligned} A_{\text{overlap}} &= A_1 + A_2 \\ &= r^2(x) \cdot \cos^{-1}\left(d_1/r(x)\right) - z \cdot d_1 \\ &\quad + r_{\text{rot}}^2 \cdot \cos^{-1}\left((d-d_1)/r_{\text{rot}}\right) - z \cdot (d - d_1) \\ &= r^2(x) \cdot \cos^{-1}\left(d_1/r(x)\right) \\ &\quad + r_{\text{rot}}^2 \cdot \cos^{-1}(d_2/r_{\text{rot}}) - z \cdot d. \end{aligned} \tag{19}$$

As shown in Fig. 6, when $d = d_1 - d_2$,

$$\begin{aligned} A_{\text{overlap}} &= A_1 + A_2 \\ &= r^2(x) \cdot \cos^{-1}\left(d_1/r(x)\right) - z \cdot d_1 \\ &\quad + r_{\text{rot}}^2 \left(\pi - \cos^{-1}\left((d_1 - d)/r_{\text{rot}}\right)\right) + z \cdot (d_1 - d) \\ &= r^2(x) \cdot \cos^{-1}\left(d_1/r(x)\right) \\ &\quad + r_{\text{rot}}^2 \left(\pi - \cos^{-1}(d_2/r_{\text{rot}})\right) + z \cdot d. \end{aligned} \tag{20}$$

III. Wind Farm Layout by Using GA

GA was inspired by the natural evolution of species. It simulates biological genes, merit-based selection, crossover, and mutation capabilities and uses the alternation of generations to produce better offspring. Therefore, the optimization problem that needs to be solved can be changed into a chromosomal and genetic model and use it to create multiple chromosomes. Then, it uses the selection, crossover, and mutation processes to find the optimal solution.

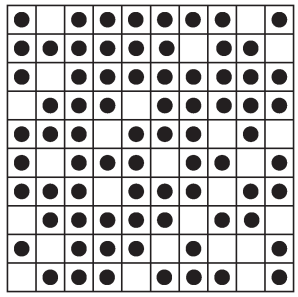

Fig. 7. Case for a random wind turbine construction diagram.

A. Encoding and Decoding

In this study, the chromosome string is a fixed wind farm area and a fixed number of wind turbines. Assuming that the extent of the wind farm area is a 10×10 matrix and there are 75 wind turbines, then the content of the chromosome is to establish 75 wind turbines in the 10×10 matrix. The horizontal spacing and vertical spacing are all five times the diameter of the wind turbine blades, as shown in Fig. 7.

B. Random Replication

Following the aforementioned chromosome string constraints, it produces a set number of chromosomes. Assuming that the number of chromosomes is set to 500, the equation will generate five hundred 10×10 matrices with each matrix containing 75 randomly constructed wind turbines.

C. Fitness Value

For the GA, the fitness value, also called the target value, is primarily used to assess the quality of each pair of chromosomes during the evolution of each generation. The higher the fitness value, the more its chromosome fits the environment, which means that it is better. Using the aforementioned system as an example, to build a fixed number of wind turbines within a limited area in a wind farm, its target value should be the optimum wind farm power generation efficiency. Equation (21) is used to calculate the total power generation in a wind farm considering wake effect, and (22) is the wind farm's efficiency

$$P_{\text{wf}} = \sum_{i=1}^{\text{NT}} P_i \tag{21}$$

$$\text{AE} = P_{\text{wf}}/P \times \text{NT} \tag{22}$$

where P_{wf} is the total power generation output in a wind farm, NT is the number of wind turbines, AE is the wind farm efficiency, and P is the rated capacity of a single wind turbine. The higher the efficiency is, the better the fitness value is.

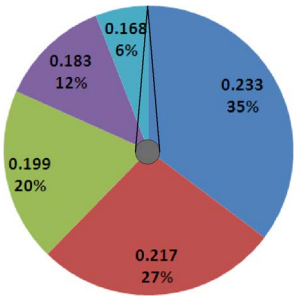

Fig. 8. Rotary-style screening schematic diagram.

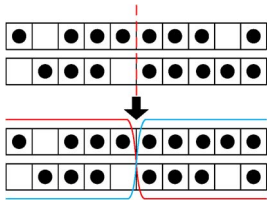

Fig. 9. Single-point crossover.

D. Replication

Replication behavior is a computing process based on the size of the fitness function in the chromosome string value to decide whether the next generation should be discarded or reproduced. There will be mass replication of the next generation if the degree of fitness is high; a low degree of fitness will be discarded. The replication process is usually a rotary-style screening. Its main function is to preserve chromosomes with good fitness values and discard the remainder by using a probability model. Using this study as an example, assume that there are five wind farms with a screening rate of 0.6; then, three wind farms will be retained. For example, if the individual power generation of each of the five wind farms is 183, 169, 215, 200, and 155 MW, respectively, with a total of 922 MW, then the probability of each individual wind farm can be calculated as 0.199, 0.183, 0.233, 0.217, and 0.168, respectively, as shown in Fig. 8. After screening, the rest of the wind farms will be eliminated.

E. Crossover

The mechanism of crossover is the focus of the entire GA, and its role is to execute the partial crossover of reproduced chromosomes in the form of pairing. The process of crossover involves the random selection of two strings (now called parent generation) to form a new string through the exchange of genes (bit data). The crossover process can be divided into single-point crossover, two-point crossover, and other methods. The two crossover methods utilized by this study are single-point crossover and two-point crossover, as shown in Figs. 9 and 10, respectively.

F. Mutation

Mutation is a method mainly used to avoid falling into a local optimum value. For example, if a wind farm consists of 75 wind turbines and a mutation rate of 0.08 is given, thus the number of wind turbines for mutation is $75 \times 0.08 = 6$. That is, six sites that do not establish wind turbines are randomly selected and exchanged with six sites with wind turbines.

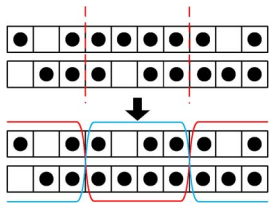

Fig. 10. Two-point crossover.

G. Optimum Solution

Each generation has a contemporary optimal solution, and this generation's optimal solution will be compared with the next generation's optimal solution. If the next generation's optimal solution is better than the previous generation's optimal solution, then it will replace the previous generation's optimal solution as the newest optimal solution. Conversely, the previous generation will be retained until all generations end, and the resulting optimal solution is the global optimal solution.

IV. Planning on the Internal Line Connection Topology by Using ACS

By following the ant system (AS) concept, Dorigo and Gambardella proposed the ACS in 1997. In this study, the state transition rules in ACS are shown in the following, where j is the next wind turbine that will be selected by ant k and S is the next wind turbine that will be randomly selected by the roulette-style method from $Jk(i)$, which is the set of wind turbines that can be linked by ant k positioned on wind turbine i:

$$j = \begin{cases} \arg \max\limits_{u \in Jk(i)} \left\{ [\tau_{iu}]^{\alpha} \times [\eta_{iu}]^{\beta} \right\}, & \text{if } q \le q_0 \\ S, & \text{otherwise} \end{cases} \tag{23}$$

where q is a random variable and has a value between zero and one that is evenly distributed, q_0 is a predetermined parameter $(0 \le q_0 \le 1)$, τ_{ij} is the pheromone concentration between wind turbines i and j, η_{ij} is the inverse of the distance between wind turbines i and j, α and β are the parameters to decide the relative importance of pheromone versus distance, the role of arg is to take the maximum product u from τ_{iu}^{α} and η_{iu}^{β}, and S will be decided by

$$P_{ij}^{k} = \begin{cases} \dfrac{[\tau_{ij}(t)]^{\alpha} \times [\eta_{ij}(t)]^{\beta}}{\sum_{k \in \text{allowed}_k} [\tau_{ij}(t)]^{\alpha} \times [\eta_{ij}(t)]^{\beta}}, & \text{if } j \in \text{allowed}_K \\ 0, & \text{otherwise.} \end{cases} \tag{24}$$

The probabilities of each wind turbine in $Jk(i)$ being selected are shown in (24).

When AS is utilized, it updates the pheromones on all the paths walked by the ants. However, ACS only updates the shortest path found by all of the ants, and its purpose is to highlight the difference between optimal solutions and other

possible solutions in that generation. All of ACS's updating rules are shown in

$$\tau_{ij} = (1-\sigma) * \tau_{ij} + \sigma * \Delta\tau_{ij} \tag{25}$$

where σ is the pheromone decaying parameter.

Additionally, the concept of "local pheromone updating rule" was added into ACS. That is, when each ant selects the next path, the pheromone for that path will be updated. The local pheromone updating rule is shown in

$$\tau_{ij} = (1-\rho) * \tau_{ij} \tag{26}$$

where ρ is the pheromone decaying parameter.

The main purpose of the local pheromone updating rule is to prevent creating an overly strong path that will attract all ants to choose it, thus avoiding confining the ants to a narrow range.

In order to make the line loss and the cost of cable construction to be considered on the same basis, this study converts the line loss into the reduced financial income of power generation. The converting procedure is as follows: First, the cable impedance in a unit length is assumed as

$$Z_d = R_d + jX_{L,d} \tag{27}$$

$$\theta_d = \tan^{-1}\left(\frac{jX_{L,d}}{R_d}\right) \tag{28}$$

where d indicates the cables with different line capacities and θ_d is the phase difference between real power and reactive power. The power generated by wind turbine i and its output current are denoted as follows:

$$P_i = VI_i \cos\theta_d \tag{29}$$

$$I_i = \frac{P_i}{V\cos\theta_d} \tag{30}$$

where V indicates the cable's rated voltage. Hence, the power loss per meter from wind turbine i to wind turbine j can be denoted as follows:

$$P_{\text{loss},ij} = I_{ij}^2 R_d. \tag{31}$$

The operating financial income from wind turbine i to wind turbine j can be denoted as

$$\text{Cost}_{\text{income},ij} = (P_{ij} - (P_{\text{loss},ij} \times l_{ij})) \times \text{Cost}_{\text{wholesale}} \times \text{Year}_{\text{wholesale}} \tag{32}$$

where l_{ij} indicates the distance between wind turbine i and wind turbine j, $\text{Cost}_{\text{wholesale}}$ is the price for the wholesale purchase of Taiwan's offshore wind power (NT$/kWh), and $\text{Year}_{\text{wholesale}}$ is the period of the wholesale purchase.

In addition to the consideration for the line loss, the cost of constructing cables is also a key factor for the optimization of the wind farm layout. This study assumes $\text{Cost}_{\text{line},ij}$ as the cost of cable construction from wind turbine i to wind turbine j, as shown in the following, of which Cost_d indicates the cost of the cables per meter with different line capacities:

$$\text{Cost}_{\text{line},ij} = l_{i,j} \times \text{Cost}_d. \tag{33}$$

TABLE II
PARAMETERS OF THE ENERCON E-101 WIND TURBINE

Number of blade	3
Rated Power	3050 kW
Rotor Diameter	101 m
Height of hub	99 m
Swept Area	8012 m^2

TABLE III
CABLE PARAMETERS IN THIS STUDY

Cable Type	A	B	C	D	E
Line diameter (mm^2)	100	200	325	400	500
Capacity (MVA)	3.47	6.78	11.06	13.77	16.76
Cost (NTD/km)	446,000	658,000	1,035,000	1,226,000	1,444,000
R (Ω/km) (20℃)	0.178	0.0923	0.0570	0.04646	0.03905
X_L (Ω/km) (20℃)	0.1882	0.1686	0.1601	0.1548	0.1502

Hence, the net financial income in the cable from wind turbine i to wind turbine j is as follows:

$$\text{Cost}_{\text{net},ij} = \text{Cost}_{\text{income},ij} - \text{Cost}_{\text{line},ij}. \tag{34}$$

The lower the value of $\text{Cost}_{\text{net},ij}$ is, the lower the net financial income in line $i-j$ will be. Equation (34) can therefore be brought into (24), and the parameter of η_{ij} in the probability equation can be converted as shown in the following, where η_{ij} is represented by a per-unit value:

$$\eta_{ij} = \text{Cost}_{\text{net},ij}. \tag{35}$$

V. DETAILED PARAMETERS FOR THE WIND FARM ARCHITECTURE IN THIS STUDY

In this paper, an 8×8 square matrix wind farm architecture will be taken as an example. The maximum number of wind turbines in this wind farm is 64. The spacing between turbines is assumed to be five times the diameter of the turbine blade. The turbine module adopts the model of Enercon E-101 wind turbine. Table II indicates the parameters of this wind turbine. The parameters used for the submarine cables are indicated in Table III, which are provided by Taiwan Power Company. The adopted wind speed time series and its probability distribution are shown in Figs. 11 and 12, respectively, which are the actual measurement data. In the Taiwan Strait, the wind direction is very stable, i.e., northeast–southwest direction, so the fixed wind direction is assumed in this study.

Additionally, the current price for the wholesale purchase of Taiwan's offshore wind power is 5.56 kWh with a period of 20 years. In this study, these actual parameters will be taken into consideration as important factors for constructing the optimal wind farm layout.

In this work, the inputs to this system are wind speed, wind direction, type of wind turbine, distance between wind turbines, number of wind turbines, specifications of cables, parameters

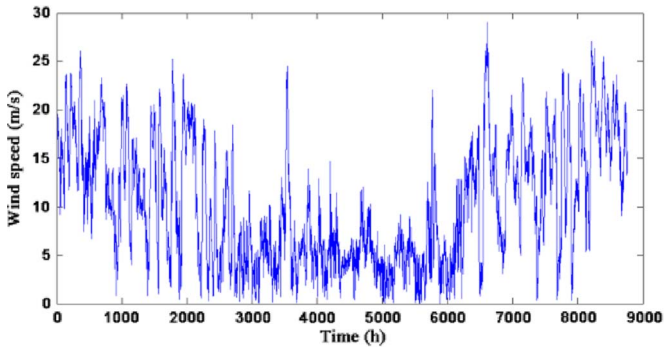

Fig. 11. Wind speed time series in a year.

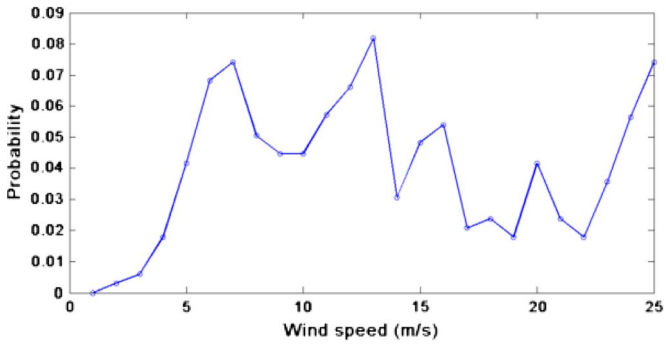

Fig. 12. Probability distribution of wind speed in a year.

of the GA and the ACS algorithm, and wholesale price of electricity by year from wind power in Taiwan. The output of the analysis is the net financial income, which concerns power generation, line losses, and the cost of investing in cables.

VI. Simulation Results

This study proposes a hybrid method combining GA and ACS to build the optimal wind farm layout. At first, several initial wind farms are built by the GA; then, the generation output from each wind turbine is calculated by considering the wake effect. Next, the parameters of each wind farm are substituted into the ACS algorithm to obtain the optimal internal cable connection by considering line length, loss, and installed cost. The ACS algorithm is suitable to find the optimal internal cable connection because of its good characteristics on the route selection. The fitness value obtained from the ACS algorithm will be back to the GA, and the optimal wind farm layout can be obtained through replication, crossover, and mutation processes of the GA. Fig. 13 shows the flowchart of the proposed method. The objective of this proposed algorithm is to find the highest net financial income for the offshore wind farm.

The parameter settings for the GA in this study include the following: The iteration number is 200 generations, there are 32 wind turbines and 200 wind farms for each generation, the screening rate is 0.5, the crossover rate is 0.6, the mutation rate is 0.05, the wake decay constant adopts a sea terrain of 0.04, and the air density is 1.225 $\mathrm{kg/m^3}$. Additionally, the parameter settings of the ant colony algorithm from (23) to (26) in this paper are as follows: The iteration number is 5000 generations, the initial τ value is one, the α value is 0.5, the β value is one, the ρ value is 0.5, and the σ value is 0.6.

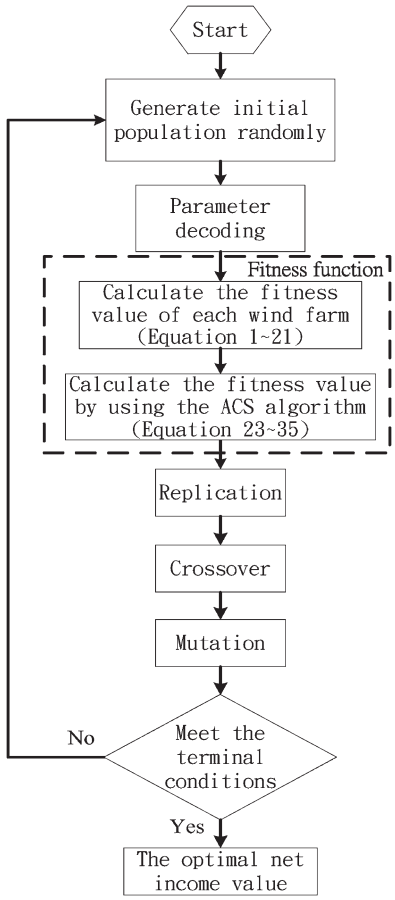

Fig. 13. Flowchart of the proposed method.

Based on our research, the combination for the line connection topology exceeds that for wind turbine location. In this work, the GA and the ACS algorithm were utilized to optimize the locations of wind turbines and the line connection topology, respectively; therefore, the number of iterations of GA is 200, which is much lower than the number of iterations of ACS (5000). Clearly, better solutions could be obtained by increasing the number of iterations of the ACS or GA. However, according to our experience, the optimal solution can almost be obtained using the aforementioned numbers of iterations. Therefore, 200 iterations for GA or 5000 iterations for ACS are enough to solve such a problem.

Fig. 14 shows the wind farm layout after adopting the GA for the optimization, and Fig. 15 shows the iteration curve in the optimization process of the GA. One can see that the GA almost finds the optimal solution for reaching the maximum output of the wind farm power around the 600th generation.

To prove that the obtained wind farm layout (Fig. 14) by using GA optimization is better than traditional manually designed wind farms, this study uses the two typical manually built wind farms in Fig. 16(a) and (b) as the comparison case. Table IV shows the comparison of average hourly power output and efficiency among the three wind farm layouts. It can be seen from Fig. 16 that the wind turbines in the artificially designed wind farms are more regularly arranged; however, since the impact of the wake effect is not really considered in them, it results in increasing loss of the overall wind power and finally

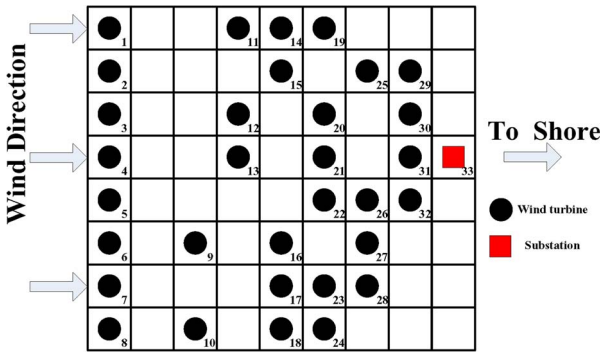

Fig. 14. Optimal wind farm layout by using the proposed method.

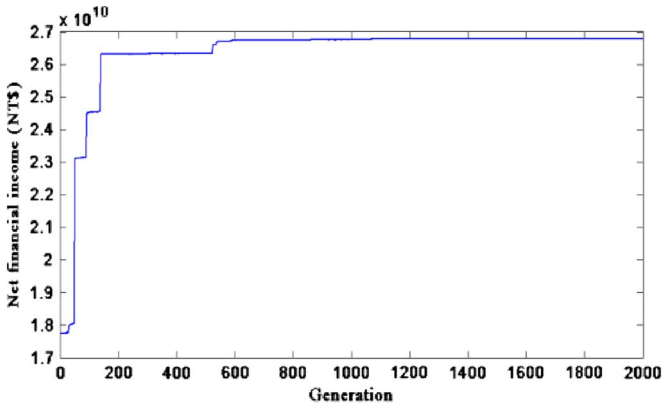

Fig. 15. Iteration curve in the optimization process of the GA.

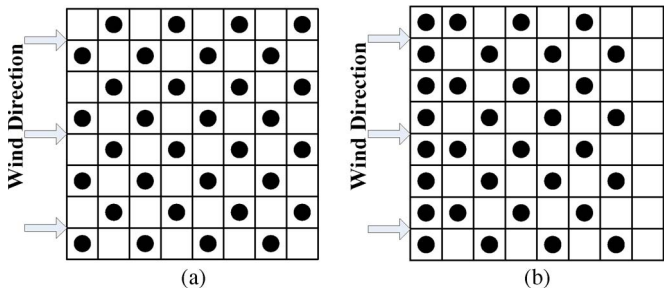

Fig. 16. Two typical cases for manually designed wind farms.

decreasing efficiency of the wind farms. By contrast, Fig. 14 seems not to be arranged very regularly; it could, however, effectively reduce the impact of the wake effect and achieve the maximum output of wind farm power.

If the 20-year wholesale purchase of wind power is considered, then the financial incomes in the three cases are as calculated. These are also shown in Table IV. The table clearly shows that the difference between financial incomes becomes large when the long-term operation of the wind farm is considered. Therefore, the proposed method still provides a considerable improvement over the artificial designs in terms of wind power generation and, correspondingly, financial income.

After obtaining the optimal arrangement structure for turbines in the wind farm, this study further adopts the ant colony algorithm to optimize the internal line connection of the wind farm. The optimal layout of an offshore wind farm depends strongly on network topology, wind speed, wind direction, and

TABLE IV
COMPARISON AMONG TWO ARTIFICIALLY DESIGNED WIND FARMS AND THE PROPOSED WIND FARM BY USING GA

Output \ Type	Artificially design wind farm 1	Artificially design wind farm 2	The proposed wind farm
Average hourly active Power (MW)	41.826	41.986	42.631
Efficiency (%)	42.85	43.02	43.68
Financial income (US $) for 20 years	1,358,106,950	1,363,302,214	1,384,245,622

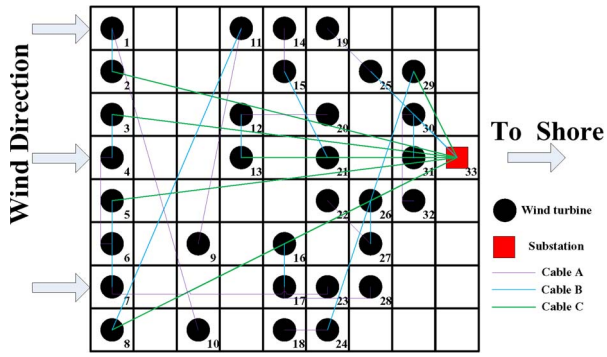

Fig. 17. Optimal layout and line connection.

other factors. For example, the number of wind turbines in a string for radial topology affects the wind power output. An understanding of the effect of the number of wind turbines in a string on the generation output of the wind farm is crucial. Therefore, in the revised paper, a sensitivity analysis with various numbers of wind turbines in a string is carried out, and the results are shown in the Appendix. Based on the simulation results, three wind turbines in a string maximize the net income. Fig. 17 shows the result for the optimal cable connection. The detailed information for the cable connection is listed in Table VII.

Generally, for wind farm topology, the length of the line with large line diameter is considered to be shorter because of its high cost. However, according to our simulation results, the suggested installed cable with large diameter is longer. That is because the large-diameter cable line has a relatively lower transmission loss. Considering the wind farm operation for two decades and comparing the initial installed costs, the impact of the line loss on the overall cost of cables will be greater. Hence, a longer low-loss cable should be used, and this suggestion also can be verified by the simulation results attained from the ant colony algorithm.

The 8×8 matrix wind farm is used in this paper as an example. It includes 32 wind turbines (the wind farm capacity is assumed 100 MW in this paper) in a fixed area. The algorithm proposed in this paper can be actually applied and extended to the optimal wind farm architecture under various environmental conditions and different numbers of turbines.

TABLE V
OPTIMAL LINE CONNECTION WITH FIVE WIND TURBINES IN A STRING

Cable Type	A		B		C		D		E	
Diameter (mm^2)	100		200		325		400		500	
	From	To	From	To	From	To	From	To	From	To
Feeder1	27	23	26	27	32	26	31	32	33	31
Feeder2	15	19	20	15	25	20	30	25	33	30
Feeder3	29	16	24	29	22	24	21	22	33	21
Feeder4	14	18	11	14	12	11	13	12	33	13
Feeder5	4	7	2	4	1	2	33	1		
Feeder6	28	17	10	28	8	10	33	8		
Feeder7	6	9	5	6	3	5	33	3		

TABLE VI
OPTIMAL LINE CONNECTION WITH FOUR WIND TURBINES IN A STRING

Cable Type	A		B		C		D	
Diameter (mm^2)	100		200		325		400	
	From	To	From	To	From	To	From	To
Feeder1	29	25	30	29	31	30	33	31
Feeder2	26	32	27	26	22	27	33	22
Feeder3	18	24	19	18	15	19	33	15
Feeder4	20	14	21	20	12	21	33	12
Feeder5	6	7	3	6	2	3	33	2
Feeder6	23	17	16	23	13	16	33	13
Feeder7	9	28	5	9	4	5	33	4
Feeder8	10	11	8	10	1	8	33	1

VII. CONCLUSION

This paper has explored how to optimize the arrangement of wind turbines in an offshore wind farm under certain regional conditions in order to produce the maximum wind power output and to conduct an optimization analysis of the cable configuration within the wind farm for reaching the optimization cost for the internal line connection in the wind farm. This paper considers the loss of wind power caused by the wake effect among turbines and explores the optimization of the wind farm arrangement through the GA to minimize the loss of wind power. In terms of the research on the internal line connection topology in the wind farm, this study adopts the most commonly used radiation connection mode and uses cables with different diameters in order to enable the research results to be consistent with the real situations. Finally, the ant colony algorithm is applied to the research of circuit configuration to optimize the cost of the circuit configuration.

From the simulation results, one can recognize that the efficiency of using artificial intelligence for arranging wind turbines and cable connections is apparently higher than manual planning because artificial intelligence algorithms can calculate the possible distribution of a large amount of cases and search the optimal solution. Many countries begin to build large-scale wind farms or reconfigure existing wind farms. The concepts and methods proposed in this study can help establish more economical and efficient offshore wind farms in the world.

APPENDIX

The number of wind turbines in a string for the radial-type topology could have an impact on wind power output. Tables V–VIII show the optimal solutions on line connection if different numbers of wind turbines are connected in a string. Each numeral in these tables indicates the site of each wind turbine, which is represented in Fig. 14. Fig. 18 shows the result of the sensitivity analysis. According to the simulation results, the construction with three wind turbines in a string can obtain the highest net income compared to the other cases.

TABLE VII
OPTIMAL LINE CONNECTION WITH THREE WIND TURBINES IN A STRING

Cable Type	A		B		C	
Diameter (mm^2)	100		200		325	
	From bus	To bus	From bus	To bus	From bus	To bus
Feeder 1	4	6	3	4	33	3
Feeder 2	30	32	31	30	33	31
Feeder 3	24	18	29	24	33	29
Feeder 4	7	23	5	7	33	5
Feeder 5	27	22	26	27	33	26
Feeder 6	15	14	21	15	33	21
Feeder 7	12	20	13	12	33	13
Feeder 8	11	9	8	11	33	8
Feeder 9	1	10	2	1	33	2
Feeder10	17	28	16	17	33	16
Feeder11	25	19	33	25	-	-

TABLE VIII
OPTIMAL LINE CONNECTION WITH TWO WIND TURBINES IN A STRING

Cable Type	A		B	
Diameter (mm^2)	100		200	
	From	To	From	To
Feeder1	31	30	33	31
Feeder2	29	25	33	29
Feeder3	32	26	33	32
Feeder4	1	2	33	1
Feeder5	20	21	33	20
Feeder6	22	16	33	22
Feeder7	13	12	33	13
Feeder8	11	10	33	11
Feeder9	18	15	33	18
Feeder10	24	14	33	24
Feeder11	4	5	33	4
Feeder12	9	17	33	9
Feeder13	27	23	33	27
Feeder14	8	6	33	8
Feeder15	3	28	33	3
Feeder16	7	19	33	7

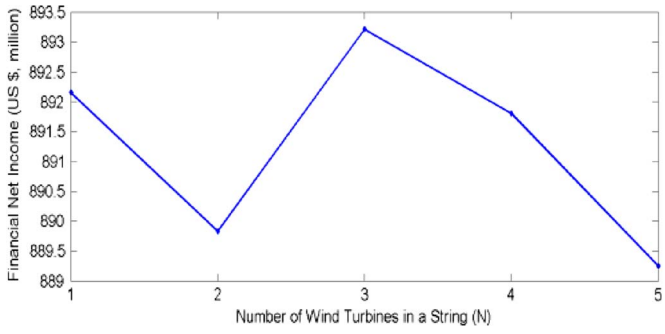

Fig. 18. Effect of different wind turbine numbers in a string on the financial net income.

REFERENCES

[1] R. Leutz, T. Ackermann, A. Suzuki, A. Akisawa, and T. Kashiwagi, "Technical Offshore Wind Energy Potentials Around the Globe," in *Proc. Eur. Wind Energy Conf.*, Copenhagen, Denmark, Jul. 2001, pp. 789–792.

[2] P. Fuglsang and K. Thomsen, "Cost optimization of wind turbines for large scale off-shore wind farms," Risoe National Laboratory, Roskilde, Denmark, Tech. Rep., 1998.

[3] J. S. Gonzalez, T. G. Rodriguez, J. C. Mora, M. Burgos Payan, and J. R. Santos, "Overall design optimization of wind farms," *Renewable Energy*, vol. 36, no. 7, pp. 1973–1982, Jul. 2011.

[4] M. Banzo and A. Ramos, "Stochastic optimization model for electric power system planning of offshore wind farms," *IEEE Trans. Power Syst.*, vol. 26, no. 3, pp. 1338–1348, Aug. 2011.

[5] J. S. Gonzalez, M. B. Payan, and J. M. Riquelme-Santos, "Optimization of wind farm turbine layout including decision making under risk," *IEEE Syst. J.*, vol. 6, no. 1, pp. 94–102, Mar. 2012.

[6] H. Hunter, C. Gary, W. Ping-Kui, W. Tien-Chieh, and S. Huai-Che, "A study of submarine power grid planning for offshore wind farm," in *Proc. IEEE Power Energy Soc. Gen. Meet.*, 2011, pp. 1–5.

[7] Z. Menghua, C. Zhe, and B. Freede, "Generation ratio availability assessment of electrical systems for offshore wind farms," *IEEE Trans. Energy Convers.*, vol. 22, no. 3, pp. 755–763, Sep. 2007.

[8] S. Dutta and T. J. Overbye, "Optimal wind farm collector system topology design considering total trenching length," *IEEE Trans. Sustain. Energy*, vol. 3, no. 3, pp. 339–348, Jul. 2012.

[9] S. Dutta and T. J. Overbye, "A clustering based wind farm collector system cable layout design," in *Proc. IEEE Power Energy Conf.*, 2011, pp. 1–6.

[10] M. Zhao, Z. Chen, and F. Blaabjerg, "Optimisation of electrical system for offshore wind farms via genetic algorithm," *IEEE Trans. Renewable Power Gen.*, vol. 3, no. 2, pp. 205–216, Jun. 2009.

[11] D. D. Li, C. He, and Y. Fu, "Optimization of internal electric connection system of large offshore wind farm with hybrid genetic and immune algorithm," in *Proc. 3rd Int. Conf. Elect. Utility Deregulation Restruct. Power Technol.*, 2008, pp. 2476–2481.

[12] M. Zhao, Z. Chen, and J. Hjerrild, "Analysis of the behaviour of genetic algorithm applied in optimization of electrical system design for offshore wind farms," in *Proc. 32nd IEEE Annu. Conf. Ind. Electron.*, 2006, pp. 2335–2340.

[13] H. Lingling, F. Yang, and G. Xiaoming, "Optimization of electrical connection scheme for large offshore wind farm with genetic algorithm," in *Proc. Int. Conf. Sustain. Power Gen. Supply*, 2009, pp. 1–4.

[14] H. S. Huang, "Distributed genetic algorithm for optimization of wind farm annual profits," in *Proc. Int. Conf. Intell. Syst. Appl. Power Syst.*, 2007, pp. 1–6.

[15] L. Dong Dong, H. Chao, and S. Hai Yan, "Optimization of electric distribution system of large offshore wind farm with improved genetic algorithm," in *Proc. IEEE Power Energy Soc. Gen. Meet. – Convers. Del. Electr. Energy 21st Century*, 2008, pp. 1–6.

[16] L. Ekonomou, S. Lazarou, G. E. Chatzarakis, and V. Vita, "Estimation of wind turbines optimal number and produced power in a wind farm using an artificial neural network model," *Simul. Modelling Practice Theory*, vol. 21, no. 1, pp. 21–25, Feb. 2012.

[17] C. Wan, J. Wang, G. Yang, H. Gu, and X. Zhang, "Wind farm micro-siting by Gaussian particle swarm optimization with local search strategy," *Renewable Energy*, vol. 48, pp. 276–286, 2012.

[18] J. Serrano Gonzalez, M. Burgos Payan, and J. M. Riquelme Santos, "An improved evolutive algorithm for large offshore wind farm optimum turbines layout," in *Proc. IEEE Trondheim Power Tech.*, 2011, pp. 1–6.

[19] K. Veeramachaneni, M. Wagner, U.-M. O'Reilly, and F. Neumann, "Optimizing energy output and layout costs for large wind farms using particle swarm optimization," in *Proc. IEEE Congr. Evol. Comput.*, 2012, pp. 1–7.

[20] Y. Erolu and S. Ulusam Seçkiner, "Design of wind farm layout using ant colony algorithm," *Renewable Energy*, vol. 44, pp. 53–62, Aug. 2012.

[21] G. Mosetti, C. Poloni, and B. Diviacco, "Optimization of wind turbine positioning in large windfarms by means of a genetic algorithm," *J. Wind Eng. Ind. Aerodynamics*, vol. 51, no. 1, pp. 105–116, Jan. 1994.

[22] S. A. Grady, M. Y. Hussaini, and M. M. Abdullah, "Placement of wind turbines using genetic algorithms," *Renewable Energy*, vol. 30, no. 2, pp. 259–270, Feb. 2005.

[23] G. Shengping and J. Li, "Study on optimization of wind farm micro-layout," in *Proc. Asia-Pacific Power Energy Eng. Conf.*, 2010, pp. 1–4.

[24] J. F. Ainslie, "Calculating the flow field in the wake of wind turbines," *JH. Wind Eng. Ind. Aerodyn.*, vol. 27, no. 1-3, pp. 213–224, Jan. 1988.

[25] P. Fuglsang and K. Thomsen, "Cost optimization of wind turbines for large-scale offshore wind farms," Risoe National Laboratory, Roskilde, Denmark, Tech. Rep., 1998.

[26] I. Katic, J. Hjstrup, and N. Jensen, "A simple model for cluster efficiency," in *Proc. EWEC*, 1986, pp. 407–410.

Yuan-Kang Wu (M'06) was born in 1970. He received the Ph.D. degree in electronic and electrical engineering from the University of Strathclyde, Glasgow, U.K., in 2004.

He was a Researcher with the Industrial Technology Research Institute, Hsinchu, Taiwan, an Engineer with the Taiwan Electric Research and Testing Center, Guanyin, Taiwan, and an Associate Professor with National Penghu University of Science and Technology, Magong, Taiwan. He is currently an Associate Professor with the Department of Electrical Engineering, National Chung Cheng University, Chiayi, Taiwan, working in the areas of wind power systems, offshore wind farm planning, renewable energy forecasting techniques, power system control and management, distributed generation, and smart grid control.

Ching-Yin Lee was born in 1957. He received the B.S.E.E. degree from National Taiwan Institute of Technology, Taipei, Taiwan, in 1983, the M.S.E.E. degree from National Taiwan University, Taipei, in 1986, and the Ph.D. degree from National Taiwan University of Science and Technology, Taipei, in 1992.

He was with Northern Taiwan Telecommunications from 1979 to 1986. He has been with the Department of Electrical Engineering, National Taipei University of Technology (NTUT), Taipei, since 1986, where he was the Chairperson of the Department of Electrical Engineering from 1992 to 1995, the Dean of the Extension Education Office, the Head of the Secretary Office from 1997 to 2001, the Dean of General Affairs from 2001 to 2006, the Dean of the College of Management from 2007 to 2008, and the Vice President from 2006 to 2009. He was a Visiting Scholar with The University of Texas at Arlington, Arlington, TX, USA, from 1996 to 1997. He is currently an Honorable Professor with NTUT and a Professor with and the President of Tungnan University, Taipei. His research interests are in power system operation, particularly in voltage stability analysis, reactive power planning, contingency analysis, power quality, distributed generation, microgrid simulation, and renewable energy.

Chao-Rong Chen (SM'11) received the B.S., M.S., and Ph.D. degrees in electrical engineering from National Taiwan University, Taipei, Taiwan, in 1983, 1988, and 1991, respectively.

In August 1991, he joined National Taipei University of Technology, Taipei, as a Faculty Member, where he is currently an Associate Professor with and the Chairman of the Department of Electrical Engineering. From 1995 to 1996, he was a Visiting Scholar with the University of Washington, Seattle, WA, USA. His current research interests include power system control and stability, renewable power systems, power system protection, intelligent control, soft computing, and energy saving.

Kun-Wei Hsu received the B.S.E.E. degree from National Penghu University of Science and Technology, Magong, Taiwan, in 2010 and the M.S.E.E. degree from National Taipei University of Technology, Taipei, Taiwan, in 2012.

He joined Taiwan Power Company, Taipei, as an Engineer in 2012. His research interests include wind power forecasting and wind farm layouts.

Huang-Tien Tseng received the B.S.E.E. degree from Feng Chia University, Taichung, Taiwan, in 2011 and the M.S.E.E. degree from National Taipei University of Technology, Taipei, Taiwan, in 2013.

He joined Taiwan Semiconductor Manufacturing Company, Hsinchu, Taiwan, as an Engineer in 2013. His research interests include wind farm layouts.